THE JOURNAL OF PHYSICAL CHEMISTRY LETTERS
A JOURNAL OF THE AMERICAN CHEMICAL SOCIETY

pubs.acs.org/JPCL

Letter

Enthalpy Change from Pure Cubic Ice I_c to Hexagonal Ice I_h

Christina M. Tonauer, Keishiro Yamashita, Leonardo del Rosso, Milva Celli, and Thomas Loerting*

Cite This: *J. Phys. Chem. Lett.* 2023, 14, 5055−5060

Read Online

ACCESS | Metrics & More | Article Recommendations | Supporting Information

ABSTRACT: The preparation of pure cubic ice without hexagonal stacking faults has been realized only recently by del Rosso et al. (*Nat. Mater.* **2020**, *19*, 663−668) and Komatsu et al. (*Nat. Commun.* **2020**, *11*, 464). With our present calorimetric study on the transition from pure cubic ice to hexagonal ice we are able to clarify the value of the enthalpy change $\Delta H_{c\rightarrow h}$ to be -37.7 ± 2.3 J mol^{-1}. The transition temperature is identified as 226 K, much higher than in previous work on ice I_{sd}. This is due to a catalytic effect of hexagonal faults on the transition, but even more importantly due to a relaxation exotherm that was not properly identified in the past.

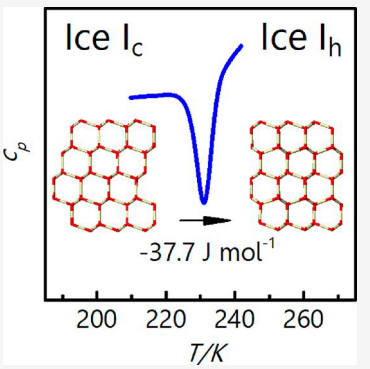

Cubic ice (I_c) was first proposed by König in 1943,[1] but its first successful experimental preparation was achieved only recently.[2,3] This metastable polytype of ice I differs from stable hexagonal ice (I_h) in terms of the stacking arrangement of layers of 6-membered rings of water molecules, which are connected via hydrogen bonds. While hexagonal ice shows an ABAB stacking (where A is a mirror image of B), cubic ice consists of layers in an ABCA arrangement. However, all "cubic ices" studied in the past actually contain significant numbers of hexagonal stacking faults, depending on the mother phase they crystallized from.[4] In retrospect, all these ices should have been termed stacking-disordered ice (ice I_{sd}), but not ice I_c.[5] Studying the relative stabilities between the three different ice I polytypes has so far not been possible in experiments due to the unavailability of pure ice I_c. Especially the enthalpy difference between ice I_c and ice I_h $\Delta H_{c\rightarrow h}$ is not known, but of fundamental interest. While it is settled that ice I_h is the stable phase in the bulk at atmospheric conditions, simulations on mW water by Lupi et al. show that, for very small sizes (up to 100,000 molecules), in fact ice I_{sd} is more stable than both ice I_c and ice I_h at 230 K.[6] This is rationalized in terms of entropy, specifically entropy gain through stacking-disorder, and supported by experimental work from Mayer & Hallbrucker,[7] who first showed that ice I_{sd} first nucleates from rapidly cooled liquid droplets at <200 K, before transforming to stable ice I_h. While there is considerable computational work on thermodynamic stability of the ice I polytypes, utilizing different water potentials (mW,[6,8,9] ST2,[10] TIP4P/Ice,[11−13] TIP4P/2005[14,15]) as well as *ab initio* methods,[16,17] experimental data on the Gibbs free energy, enthalpy, and entropy are notoriously difficult to access. Hondoh et al.[18,19] approached this question applying X-ray topography to study formation and annihilation of stacking faults and reported a free energy cost of 0.31 mJ m^{-2} (16.5 J mol^{-1} [6]) at 253 K, associated with the annihilation of a hexagonal stacking fault in ice I_c.

In terms of enthalpy difference, numerous calorimetric studies are available that have scrutinized the transition from different stacking-disordered ices I_{sd} to I_h, as listed in Table 1. The reported literature values for the enthalpy change scatter by an order of magnitude, ranging from less than −10 [20] to ca. −160 [21] J mol^{-1}. The difference in the reported results is not only due to the different number of hexagonal stacking faults in differently prepared variants of ice I_{sd}. Much more so, there are fundamental issues about the nature of the heat release observed in calorimetry experiments on powdered samples. This becomes obvious by comparing the different calorimetric signatures and peak integration methods. Some studies report the existence of a "pre-peak" around ∼170 K (see Table 1), prior to the polytypic transition exotherm,[22,23] often assigned to growth of crystallites, crack healing, and strain relief.[24] Other authors observe only one, "merged" exothermic feature between ∼170−240 K,[21,25−29] and some authors report both cases, depending on differences in heating rate and powdering of samples.[7,24] It has remained unclear so far, what actually causes a double-peak and what causes a merged, single peak in calorimetry experiments, where typically very slow heating on the order of K/h was employed in Tian-Calvet calorimetry, but faster heating on the order of K/min in differential scanning calorimetry experiments. It is thus an open question, how to

Received: February 13, 2023
Accepted: May 2, 2023
Published: May 25, 2023

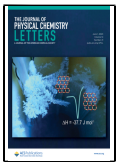

https://doi.org/10.1021/acs.jpclett.3c00408
J. Phys. Chem. Lett. 2023, 14, 5055−5060

Table 1. Comparison of Calorimetry Studies on the Ice I_{sd} to Ice I_h Transition[a]

			Pre-Peak	Ice I_{sd} → Ice I_h	
Study	Mother phase	Heating rate/K min^{-1}	T_{init}; T_{final}/K	T_{init}; T_{final}/K	$\Delta H_{sd\to h}$ /J mol^{-1}
Handa et al. (1986)[22]	uHDA	0.167	190; 219	219 ± 2; 232 ± 0	−16 ± 5
Beaumont et al. (1961)[40]	ASW	-	-	∼200	<−106 *
Sugisaki et al.(1968)[21]	ASW	-	merged	160; 210	−161 ± 15 *
McMillan & Los (1965)[26]	ASW	16	-	∼186 (T_{onset})	−151 *
Ghormley (1968)[23]	ASW	20	193; 223	223; 268	< −20
Mayer & Hallbrucker (1987)[7]	HGW (190 K)	10	merged	∼223 (T_{min})	−56 *
	HGW (170 K)	10	2 subminima	-	−56 *
Johari et al. (1990)[27]	HGW (77 K)	30	merged	224 ± 2 (T_{min})	−50 to −60 *
Kohl et al. (2000)[24]	HGW (130 K)	30	∼193 (T_{min})	∼230 (T_{min})	−40 *
	HGW (140 K)	30	∼193 (T_{min})	∼230 (T_{min})	−36 *
	HGW (150 K)	30	∼193 (T_{min})	∼230 (T_{min})	−33
	HGW (160 K)	30	2 subminima	-	−128 *
	HGW (170 K)	30	2 subminima	-	−147 *
	HGW (190 K)	30	merged	-	−96 *
Handa et al. (1986)[28]	ice V	0.167	merged	179 ± 2; 217 ± 1	−51 ± 1 *
	ice VI	0.167	merged	177 ± 1; 217 ± 0	−50 ± 4 *
Yamamuro et al. (1987)[29]	III, IX	0.042	3 subminima	165; 225	−37 ± 1 *
Handa et al. (1988)[25]	II	0.167	merged	186 ± 6; 227 ± 3	−36 ± 4
	IX	0.167	merged	179 ± 4; 230 ± 4	−13 ± 4
	VIII	0.167	merged	186 ± 0; 228 ± 0	−35 ± 1
	LDA	0.167	-	-	−35 ± 4
Salzmann et al. (2004)[41]	IV	5	-	∼216 (T_{min})	−20 ± 7
	XII	5	-	∼217 (T_{min})	−31 ± 3
Fuentes-Landete et al. (2020)[20]	II	30	-	∼210 (T_{init})	<−10

[a] T_{init} and T_{final} denote the initial and final temperature of a peak in a calorimetric scan, respectively, i.e., the integration limits for determination of the enthalpy change. T_{onset} and T_{min} represent the temperatures at the onset and the minimum of an exothermic feature, respectively, as shown in Figure 1a. "Merged" implies that the pre-peak overlaps with the main peak for the ice I_{sd} to ice I_h transition. Based on the results of the present study, we mark enthalpy values that were likely overestimated in literature by (*).

properly integrate the peaks. This question has to be addressed together with the differing cubicity in ice I_{sd},[30,31] i.e., different numbers of hexagonal stacking faults for differently prepared forms of ice I_{sd}. In the present work we make use of a fully cubic sample, so that differing cubicity is no longer an issue, and so that we are able to assign the prepeak to relaxation phenomena unrelated to the actual rearrangement from cubic to hexagonal stacking sequences. That is, with the experimental accessibility of pure cubic ice (crystallized from ice XVII[2] or hydrogen hydrate[3]), this study is aimed at the open question about the enthalpy difference between ice I_c and ice I_h, $\Delta H_{c\to h}$.

In addition to the relevance for thermodynamics of ice I polytypes, this study has further implications for our understanding of fundamental processes in Earth's atmosphere, e.g., the formation of cold cirrus clouds in the upper troposphere[32] or noctilucent/polar mesospheric clouds (PMCs) at even higher altitudes in Earth's mesosphere (∼80 km).[33] While there has been consensus that ice I_{sd} exists in Earth's atmosphere in addition to predominant ice I_h,[34−38] likely based on preferential formation of small stacking-disordered crystallites via homogeneous nucleation,[6] a recent study has shown that cubic ice crystallites preferentially form via heterogeneous nucleation on graphene or h-BN at ∼110 K,[39] a plausible mechanism at mesospheric conditions.

We here present differential scanning calorimetry (DSC) measurements of the cubic to hexagonal ice transition, starting from pure H_2O cubic ice transformed from XVII, that is, void of hexagonal stacking faults.[2]

Figure 1a depicts one representative heating scan of a sample of ice I_c between 160 and 250 K. Figure 1b shows a powder X-ray diffractogram of a sample of cubic ice at 80 K, with sample holder peaks marked by asterisks. The three intense Bragg peaks at 24.19°, 40.02°, and 47.31°, representing the 111, 220, and 311 reflexes, show that the sample under scrutiny is ice I_c. For stacking-disordered hexagonal ice the 111 peak is usually significantly broadened and shows a shoulder at ∼22.8° which originates from hexagonal stacks. In our case, there is a tiny peak at ∼23.00°, where the intensity is less than 3% of the 111 Bragg peak intensity. Other Bragg peaks of ice I_h are below the noise level of the measurement (positions marked by crossed gray arrows, taken from ref 42), which indicates that no hexagonal ice has condensed from air onto the sample. That is, there is a very small inherent amount of hexagonal stacking faults in our pure cubic ice. For comparison, "cubic ices" studied in the past prepared from other mother phases, e.g., from high-pressure ice polymorphs, from amorphous ice, or from the liquid, feature an intensity of the 100 Bragg peak of ice I_h at least an order of magnitude larger than seen in Figure 1b. This is why we follow the literature practice to call this ice "pure" ice I_c, essentially void of ice I_h.

The thermogram $c_p(T)$ in Figure 1a recorded using a heating rate of 30 K min^{-1} clearly shows that the I_c to I_h transition appears as a sharp exothermic feature centered around 231 K, with an onset temperature T_{onset} of 226 K (determined by the intersection of two straight lines extrapolating the baseline and the peak edge of the exotherm, respectively, see SI Table 1). The integration of this peak (within the limits of 221 and 240 K, sketched by the red dashed baseline) yields the enthalpy of transition from cubic to hexagonal ice.

https://doi.org/10.1021/acs.jpclett.3c00408
J. Phys. Chem. Lett. 2023, 14, 5055−5060

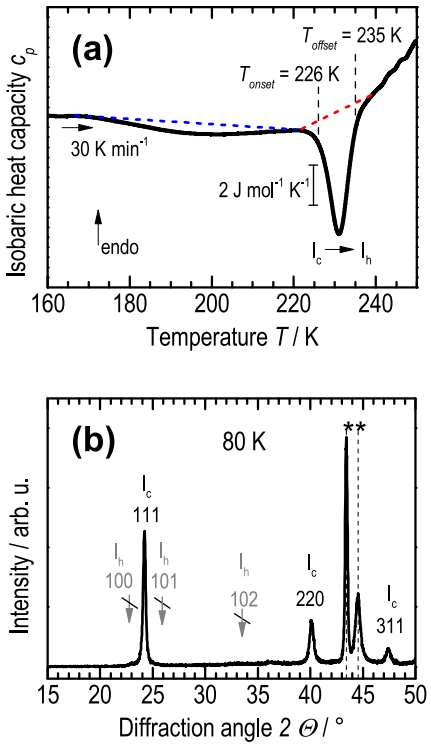

Figure 1. (a) Thermogram $c_p(T)$ of a heating scan (after baseline correction) of a sample of pure cubic ice showing the sharp and well-separated I_c to I_h transition exotherm centered around 231 K. (b) Powder X-ray diffractogram of pure cubic ice at 80 K, showing only 3 characteristic Bragg peaks at 24.19° (3.676 Å), 40.02° (2.251 Å), and 47.31° (1.920 Å) characteristic for ice I_c.[2] As a reference, the positions of characteristic Bragg peaks of ice I_h at 22.79° (3.899 Å), 25.80° (3.442 Å), and 33.62° (2.670 Å) are marked by crossed gray arrows.[42] Sample holder peaks are marked by asterisks. Diffraction angles at *x*-axis correspond to Cu Kα radiation.

$$\Delta H_{c\rightarrow h} = -37.7 \pm 2.3 \text{ J mol}^{-1}$$

(Average of 9 independent measurements, standard error given as standard deviation based on a sample of the population, see SI Table 1).

We emphasize that the transition starts from hydrogen-disordered ice I_c and ends in hydrogen-disordered ice I_h. That is, there is no entropy difference between the two ices in terms of hydrogen order. Hydrogen ordering in ice I is of relevance only below 72 K.[43] Our enthalpy difference compares with a calculated difference of 0 ± 30 J mol^{-1} in mW water.[44] Considering the free energy change $\Delta G_{c\rightarrow h} = -16.5$ J mol^{-1} measured by Hondoh,[18,19] our result implies that cubic ice is destabilized by enthalpy but stabilized by entropy (which does not originate from Pauling entropy). In addition, we performed DSC scans of ice I_c at heating rates of 10 and 50 K min^{-1}, successively (see SI Figure 2). Applying different heating rates shows an expected effect on the onset temperatures, where T_{onset} increases with increasing heating rate (SI Figure 2) but shows no effect on $\Delta H_{c\rightarrow h}$ (see SI Table 1). Also, we measured thermograms starting from a sample of ice XVII as precursor for ice I_c (SI Figure 3). While these scans show the same transition enthalpy $\Delta H_{c\rightarrow h}$, the I_c-I_h transition is shifted to ~3 K higher onset temperatures compared to experiments starting from ice I_c. We interpret this as a result from different thermal history, once again emphasizing the metastable nature of ice I_c. Specifically, the cubic ice that forms in the course of the DSC heating scan *in statu nascendi* from ice XVII needs a bit more time to rearrange to hexagonal ice compared to pure ice I_c prepared outside the DSC instrument.

Furthermore, our heating experiments of cubic ice exhibit a broad and weak exothermic feature prior to the polytypic transition, centered around ~193 K (Figure 1a). It shows an enthalpy change of −14.4 ± 2.3 J mol^{-1} (integration limits marked by the blue dashed baseline in Figure 1a, for measured values see SI Table 2). This feature has also been reported by Kohl et al. in their calorimetry (and X-ray diffraction) study of hyperquenched glassy water (HGW)/ice I_c.[24] They assigned the weak exotherm to a relaxation phenomenon, likely composed of effects from coalescence of particles, relief of nonuniform strain, and healing of different kinds of defects. Also in case of the powder of cubic ice employed here, relaxation (probably at the grain interfaces) takes place prior to the transition itself. As evident in SI Figure 2 this feature is different for different heating rates and furthermore also different depending on whether cubic ice was made beforehand or inside the DSC instrument (compare SI Figures 2 and 3). In other words, the size of this feature depends very much on the size of ice grains and/or morphology but is not related to the actual I_c to I_h transition. Employing heating rates of 10−50 K min^{-1} allows for clear separation of the relaxation exotherm from the I_c to I_h transition in the present study. That is, the prepeak is related to the powdering of the sample, size of grains, etc., but unrelated to the inherent rearrangement of cubic to hexagonal stacking sequences.

Considering the literature data shown in Table 1, studies integrating a "merged" exothermic feature overestimate the heat release. That is, all enthalpies that are labeled "merged" in Table 1 contain a contribution from relaxation that is not related to the bulk enthalpy for the cubic-to-hexagonal transition. The "true" $\Delta H_{c\rightarrow h}$(ice I_{sd}) in these studies is less negative, closer to zero, than the apparent $\Delta H_{c\rightarrow h}$(ice I_{sd}) reported by the authors. We mark the studies which likely overestimated the enthalpy change by (*) in Table 1. For example, Handa et al.[28] performed heating scans of different samples of stacking-disordered ice I_{sd}, crystallized from ice V and ice VI, respectively, at ~0.17 K min^{-1} and observed only one exotherm between ~175 and 220 K. This can be rationalized by the low heating rate and a catalytic effect of the hexagonal stacking faults within the cubic ice sample, lowering the onset temperature of the cubic to hexagonal transition. As a result, the two exothermic events ((i) relaxation and (ii) transformation of ice I_c to ice I_h) merge to one. Therefore, the value of $\Delta H_{c\rightarrow h}$ was overestimated to be ca. −50 J mol^{-1},[28] very close to the sum of the two heats reported here. A similar catalytic effect was also found in a Raman spectroscopy study of the ice I_c-I_h transformation in the same pure cubic ice samples as studied here,[45] where an even slower heating ramp (namely, 0.037 K min^{-1}) was applied, and the transformation was completed at temperatures below 200 K. That is, even the tiny amount of hexagonal stacking faults noted in Figure 1b catalyzes the transition. Furthermore, Yamamuro et al.[29] likely reported a too-large (negative) enthalpy change, even though their value (−37 ± 1 Jmol^{-1}) coincides with the value presented here. However, in light of the present study, their integration limits were chosen too broadly. Considering their Figure 12 of ref 29, integration between ~200 and ~230 K, excluding the prepeak feature merged with the actual I_{sd}-I_h transition exotherm, seems most accurate.

https://doi.org/10.1021/acs.jpclett.3c00408
J. Phys. Chem. Lett. 2023, 14, 5055−5060

With the present finding of $\Delta H_{c\to h} = -37.7 \pm 2.3$ J mol^{-1} we finally establish clarity for the long-standing inconsistency related to the transformation enthalpy of cubic to hexagonal ice in bulk samples. This result is a benchmark for future simulations aimed at the equilibrium between liquid and crystalline water at ambient pressure.[8,10,14,16] Furthermore, this result can be applied for an approximation of the difference in vapor pressure between ice I_c (p_c) and ice I_h (p_h), a key question for supersaturation above ice clouds and the mechanism of cloud formation.[46] Based on the Clausius–Clapeyron equation, the ratio of the vapor pressures is often approximated[32] as

$$\ln \frac{p_h}{p_c} = \frac{\Delta H_{c\to h}}{RT} \quad (1)$$

Entering the value of $\Delta H_{c\to h}$ into eq 1 shows that the vapor pressure of pure ice I_c is only 3% higher than the one of ice I_h at 170 K and only 2% higher at 230 K. In terms of absolute vapor pressure of cubic ice, we can then use the vapor pressure reported for ice I_h by Marti & Mauersberger[47] as well as Mauersberger & Krankowsky.[48] Adding the 3% and 2%, the absolute vapor pressure above ice I_c calculates as 7.19×10^{-4} Pa at 170 K and 10.2×10^{-4} Pa at 230 K. The vapor pressure of ice I_{sd} particles in clouds will inevitably be between the two values, i.e., even closer to the one of ice I_h. Any form of stacking-disordered ice containing a significant amount of hexagonal stacking faults will inevitably show a less negative $\Delta H_{c\to h}$ and accordingly an even smaller difference in vapor pressure compared to pure hexagonal ice. That is, our result is inconsistent with measurements reporting a difference in vapor pressure of ∼10% between ice I_{sd} and ice I_h,[32,49] with the need of clarification and more direct measurements of the vapor pressure of ices I_c and I_{sd} in the future. Calorimetric studies providing values more negative than -37.7 ± 2.3 J mol^{-1} are affected by relaxation effects and peak merging without proper separation from the exotherm related to the transition itself (Table 1).

Moreover, the measured onset temperatures of the cubic to hexagonal ice transition of 220, 226, and 230 K at 10, 30, and 50 K min^{-1}, respectively, provide important clues for understanding which forms of ice are present in the layers of our atmosphere and how their structure influence properties such as Earth's albedo.[50−52] "Cubic ice" in our atmosphere is more stacking-faulty than the ice studied here, so it will experience an even more pronounced catalytic effect of pre-existing hexagonal stacks. For that reason, the transition from ice I_{sd} to ice I_h can take place at temperatures below 200 K. On the contrary, the uncatalyzed transition will take place at higher temperature. For pure ice I_c made from the C_2 structure of hydrogen hydrate H_2−H_2O (by complete degassing of hydrogen, resulting in the empty cubic host structure as reported by Komatsu et al.[3]) a transition temperature above 240 K was found. It would be very interesting to study a sample prepared in that manner calorimetrically, but so far such samples have not been recovered for ex situ measurements. Knowledge of the phase behavior of the different polytypes of ice I, e.g., their stability with respect to each other combined with remote sensing, will facilitate new insights of the thermal history of celestial bodies.[53]

EXPERIMENTAL METHODS

Pure ice I_c was obtained by heating a powder of ice XVII to 150 K. The precursor material ice XVII was previously obtained by means of a suitable thermal treatment of hydrogen hydrate samples in C_0 structure.[54] In total we recorded nine heating scans at 10, 30, and 50 K min^{-1} of samples of ∼10–20 mg of cubic ice in aluminum crucibles using a *DSC8000* by PerkinElmer. After the first heating scan, the sample (after transformation to ice I_h) was cooled down to ∼93 K and reheated in a second heating scan. This second scan (of ice I_h) was used for baseline correction (see SI Figure 1). The calorimetric features were normalized by the melting enthalpy of ice I_h, i.e., 6012 J mol^{-1} at 273 K. The uncertainty of measured temperatures is ±1 K (for more detail about the method and instrument calibration, see ref 55). Powder X-ray diffraction at ∼80 K and subambient pressure (∼1 mbar) using a Siemens *D5000* applying Cu Kα radiation in θ–θ geometry was performed for sample characterization prior to the DSC measurements.

ASSOCIATED CONTENT

Supporting Information

The Supporting Information is available free of charge at https://pubs.acs.org/doi/10.1021/acs.jpclett.3c00408.

SI Table 1 covers characteristic temperatures and transformation enthalpies of the ice I_c to ice I_h transition for each individual run at the indicated heating rates. SI Table 2 contains information on the relaxation exotherm prior to the polytypic ice I_c to I_h transformation (integration limits $T_{initial}/T_{final}$ and peak minimum T_{min}, as well as the enthalpy change ΔH_{relax}). SI Figure 1 depicts a typical heating scan prior to baseline correction and the applied baseline for reference. SI Figure 2 shows a comparison of (baseline corrected) DSC scans at heating rates 10, 30, and 50 K min^{-1}, respectively, pointing out a shift of T_{onset} to higher temperatures with increasing heating rate. SI Figure 3 contains two heating scans (10 and 30 K min^{-1}, respectively) starting from ice XVII (PDF)

Transparent Peer Review report available (PDF)

AUTHOR INFORMATION

Corresponding Author

Thomas Loerting − *Institute of Physical Chemistry, University of Innsbruck, A-6020 Innsbruck, Austria;* orcid.org/0000-0001-6694-3843; Email: thomas.loerting@uibk.ac.at

Authors

Christina M. Tonauer − *Institute of Physical Chemistry, University of Innsbruck, A-6020 Innsbruck, Austria;* orcid.org/0000-0001-6859-5344

Keishiro Yamashita − *Institute of Physical Chemistry, University of Innsbruck, A-6020 Innsbruck, Austria;* orcid.org/0000-0003-3215-3995

Leonardo del Rosso − *Consiglio Nazionale delle Ricerche, Istituto di Fisica Applicata 'Nello Carrara', I-50019 Sesto Fiorentino, Italy;* orcid.org/0000-0002-7134-4121

Milva Celli − *Consiglio Nazionale delle Ricerche, Istituto di Fisica Applicata 'Nello Carrara', I-50019 Sesto Fiorentino, Italy;* orcid.org/0000-0002-0537-6029

Complete contact information is available at: https://pubs.acs.org/10.1021/acs.jpclett.3c00408

Notes

The authors declare no competing financial interest.

■ ACKNOWLEDGMENTS

The authors thank Lorenzo Ulivi for the discussion and reviewing the manuscript. This research was supported by the Centre for Molecular Water Science (CMWS, DESY Hamburg) in an Early Science Project. C.M.T. received a DOC fellowship of the Austrian Academy of Sciences ÖAW and is supported by the Early Stage Funding 2021 of the University of Innsbruck. K.Y. is a recipient of an overseas research fellowship by the Japan Society for the Promotion of Science (JSPS). The authors thank Andrea Donati (IFAC−CNR) for the technical support. M.C. and L.d.R. aknowledge the support from the Fondazione Cassa di Risparmio di Firenze under the contract "Grandi Attrezzature 2019 - HYDRO10000" (2019/0244).

■ REFERENCES

(1) König, H. Eine Kubische Eismodifikation. *Z. Kristallogr.* **1943**, *105*, 279−286.
(2) del Rosso, L.; Celli, M.; Grazzi, F.; Catti, M.; Hansen, T. C.; Fortes, A. D.; Ulivi, L. Cubic Ice I_c without Stacking Defects Obtained from Ice XVII. *Nat. Mater.* **2020**, *19* (6), 663−668.
(3) Komatsu, K.; Machida, S.; Noritake, F.; Hattori, T.; Sano-Furukawa, A.; Yamane, R.; Yamashita, K.; Kagi, H. Ice I_c without Stacking Disorder by Evacuating Hydrogen from Hydrogen Hydrate. *Nat. Commun.* **2020**, *11* (1), 464.
(4) Carr, T. H. G.; Shephard, J. J.; Salzmann, C. G. Spectroscopic Signature of Stacking Disorder in Ice I. *J. Phys. Chem. Lett.* **2014**, *5* (14), 2469−2473.
(5) Malkin, T. L.; Murray, B. J.; Brukhno, A. V.; Anwar, J.; Salzmann, C. G. Structure of Ice Crystallized from Supercooled Water. *Proc. Natl. Acad. Sci. U. S. A.* **2012**, *109* (4), 1041−1045.
(6) Lupi, L.; Hudait, A.; Peters, B.; Grünwald, M.; Gotchy Mullen, R.; Nguyen, A. H.; Molinero, V. Role of Stacking Disorder in Ice Nucleation. *Nature* **2017**, *551* (7679), 218−222.
(7) Mayer, E.; Hallbrucker, A. Cubic Ice from Liquid Water. *Nature* **1987**, *325* (6105), 601−602.
(8) Hudait, A.; Qiu, S.; Lupi, L.; Molinero, V. Free Energy Contributions and Structural Characterization of Stacking Disordered Ices. *Phys. Chem. Chem. Phys.* **2016**, *18* (14), 9544−9553.
(9) Quigley, D. Communication: Thermodynamics of Stacking Disorder in Ice Nuclei. *J. Chem. Phys.* **2014**, *141* (12), 121101.
(10) Smallenburg, F.; Poole, P. H.; Sciortino, F. Phase Diagram of the ST2 Model of Water. *Mol. Phys.* **2015**, *113* (17−18), 2791−2798.
(11) Haji-Akbari, A.; Debenedetti, P. G. Direct Calculation of Ice Homogeneous Nucleation Rate for a Molecular Model of Water. *Proc. Natl. Acad. Sci. U. S. A.* **2015**, *112* (34), 10582−10588.
(12) Grabowska, J. Why Is the Cubic Structure Preferred in Newly Formed Ice? *Phys. Chem. Chem. Phys.* **2019**, *21* (33), 18043−18047.
(13) Niu, H.; Yang, Y. I.; Parrinello, M. Temperature Dependence of Homogeneous Nucleation in Ice. *Phys. Rev. Lett.* **2019**, *122* (24), 245501.
(14) Zaragoza, A.; Conde, M. M.; Espinosa, J. R.; Valeriani, C.; Vega, C.; Sanz, E. Competition between Ices I_h and I_c in Homogeneous Water Freezing. *J. Chem. Phys.* **2015**, *143* (13), 134504.
(15) Espinosa, J. R.; Vega, C.; Sanz, E. Ice−Water Interfacial Free Energy for the TIP4P, TIP4P/2005, TIP4P/Ice, and mW Models As Obtained from the Mold Integration Technique. *J. Phys. Chem. C* **2016**, *120* (15), 8068−8075.
(16) Piaggi, P. M.; Panagiotopoulos, A. Z.; Debenedetti, P. G.; Car, R. Phase Equilibrium of Water with Hexagonal and Cubic Ice Using the SCAN Functional. *J. Chem. Theory Comput.* **2021**, *17* (5), 3065−3077.
(17) Cheng, B.; Engel, E. A.; Behler, J.; Dellago, C.; Ceriotti, M. Ab Initio Thermodynamics of Liquid and Solid Water. *Proc. Natl. Acad. Sci. U. S. A.* **2019**, *116* (4), 1110−1115.
(18) Hondoh, T.; Itoh, T.; Amakai, S.; Goto, K.; Higashi, A. Formation and Annihilation of Stacking Faults in Pure Ice. *J. Phys. Chem.* **1983**, *87* (21), 4040−4044.
(19) Hondoh, T. Dislocation Mechanism for Transformation between Cubic Ice I_c and Hexagonal Ice I_h. *Philos. Mag.* **2015**, *95* (32), 3590−3620.
(20) Fuentes-Landete, V.; Rasti, S.; Schlögl, R.; Meyer, J.; Loerting, T. Calorimetric Signature of Deuterated Ice II: Turning an Endotherm to an Exotherm. *J. Phys. Chem. Lett.* **2020**, *11* (19), 8268−8274.
(21) Sugisaki, M.; Suga, H.; Seki, S. Calorimetric Study of the Glassy State. IV. Heat Capacities of Glassy Water and Cubic Ice. *Bull. Chem. Soc. Jpn.* **1968**, *41* (11), 2591−2599.
(22) Handa, Y. P.; Mishima, O.; Whalley, E. High-density Amorphous Ice. III. Thermal Properties. *J. Chem. Phys.* **1986**, *84* (5), 2766−2770.
(23) Ghormley, J. A. Enthalpy Changes and Heat-Capacity Changes in the Transformations from High-Surface-Area Amorphous Ice to Stable Hexagonal Ice. *J. Chem. Phys.* **1968**, *48* (1), 503−508.
(24) Kohl, I.; Mayer, E.; Hallbrucker, A. The Glassy Water−Cubic Ice System: A Comparative Study by X-Ray Diffraction and Differential Scanning Calorimetry. *Phys. Chem. Chem. Phys.* **2000**, *2* (8), 1579−1586.
(25) Handa, Y. P.; Klug, D. D.; Whalley, E. Energies of the Phases of Ice at Low Temperature and Pressure Relative to Ice I_h. *Can. J. Chem.* **1988**, *66* (4), 919−924.
(26) McMillan, J. A.; Los, S. C. Vitreous Ice: Irreversible Transformations During Warm-Up. *Nature* **1965**, *206* (4986), 806−807.
(27) Johari, G. P.; Hallbrucker, A.; Mayer, E. Isotope Effect on the Glass Transition and Crystallization of Hyperquenched Glassy Water. *J. Chem. Phys.* **1990**, *92* (11), 6742−6746.
(28) Handa, Y. P.; Klug, D. D.; Whalley, E. Difference in Energy between Cubic and Hexagonal Ice. *J. Chem. Phys.* **1986**, *84* (12), 7009−7010.
(29) Yamamuro, O.; Oguni, M.; Matsuo, T.; Suga, H. Heat Capacity and Glass Transition of Pure and Doped Cubic Ices. *J. Phys. Chem. Solids* **1987**, *48* (10), 935−942.
(30) Hansen, T. C.; Koza, M. M.; Kuhs, W. F. Formation and Annealing of Cubic Ice: I. Modelling of Stacking Faults. *J. Phys.: Condens. Matter* **2008**, *20* (28), 285104.
(31) Hansen, T. C.; Koza, M. M.; Lindner, P.; Kuhs, W. F. Formation and Annealing of Cubic Ice: II. Kinetic Study. *J. Phys.: Condens. Matter* **2008**, *20* (28), 285105.
(32) Shilling, J. E.; Tolbert, M. A.; Toon, O. B.; Jensen, E. J.; Murray, B. J.; Bertram, A. K. Measurements of the Vapor Pressure of Cubic Ice and Their Implications for Atmospheric Ice Clouds. *Geophys. Res. Lett.* **2006**, *33* (17), L17801.
(33) Hervig, M.; Thompson, R. E.; McHugh, M.; Gordley, L. L.; Russell, J. M.; Summers, M. E. First Confirmation That Water Ice Is the Primary Component of Polar Mesospheric Clouds. *Geophys. Res. Lett.* **2001**, *28* (6), 971−974.
(34) Whalley, E. Scheiner's Halo: Evidence for Ice I_c in the Atmosphere. *Science* **1981**, *211* (4480), 389−390.
(35) Riikonen, M.; Sillanpää, M.; Virta, L.; Sullivan, D.; Moilanen, J.; Luukkonen, I. Halo Observations Provide Evidence of Airborne Cubic Ice in the Earth's Atmosphere. *Appl. Opt.* **2000**, *39* (33), 6080.
(36) Murphy, D. M. Dehydration in Cold Clouds Is Enhanced by a Transition from Cubic to Hexagonal Ice. *Geophys. Res. Lett.* **2003**, *30* (23), 2230.
(37) Murray, B. J.; Knopf, D. A.; Bertram, A. K. The Formation of Cubic Ice under Conditions Relevant to Earth's Atmosphere. *Nature* **2005**, *434* (7030), 202−205.
(38) Murray, B. J.; Bertram, A. K. Formation and Stability of Cubic Ice in Water Droplets. *Phys. Chem. Chem. Phys.* **2006**, *8* (1), 186−192.

https://doi.org/10.1021/acs.jpclett.3c00408
J. Phys. Chem. Lett. 2023, 14, 5055−5060

(39) Huang, X.; Wang, L.; Liu, K.; Liao, L.; Sun, H.; Wang, J.; Tian, X.; Xu, Z.; Wang, W.; Liu, L.; Jiang, Y.; Chen, J.; Wang, E.; Bai, X. Tracking Cubic Ice at Molecular Resolution. *Nature* **2023**, *617*, 86−91.
(40) Beaumont, R. H.; Chihara, H.; Morrison, J. A. Transitions between Different Forms of Ice. *J. Chem. Phys.* **1961**, *34* (4), 1456−1457.
(41) Salzmann, C. G.; Mayer, E.; Hallbrucker, A. Thermal Properties of Metastable Ices IV and XII: Comparison, Isotope Effects and Relative Stabilities. *Phys. Chem. Chem. Phys.* **2004**, *6* (6), 1269.
(42) Dowell, L. G.; Rinfret, A. P. Low-Temperature Forms of Ice as Studied by X-Ray Diffraction. *Nature* **1960**, *188* (4757), 1144−1148.
(43) Geiger, P.; Dellago, C.; Macher, M.; Franchini, C.; Kresse, G.; Bernard, J.; Stern, J. N.; Loerting, T. Proton Ordering of Cubic Ice I_c: Spectroscopy and Computer Simulations. *J. Phys. Chem. C* **2014**, *118* (20), 10989−10997.
(44) Moore, E. B.; de la Llave, E.; Welke, K.; Scherlis, D. A.; Molinero, V. Freezing, Melting and Structure of Ice in a Hydrophilic Nanopore. *Phys. Chem. Chem. Phys.* **2010**, *12* (16), 4124.
(45) Celli, M.; Ulivi, L.; del Rosso, L. Raman Investigation of the Ice I_c − Ice I_h Transformation. *J. Phys. Chem. C* **2020**, *124* (31), 17135−17140.
(46) Bogdan, A.; Loerting, T. Cubic Ice and Large Humidity with Respect to Ice in Cold Cirrus Clouds. In *Geophysical Research Abstracts;* EGU General Assembly 2009, 2009; Vol. *11*, p 13419.
(47) Marti, J.; Mauersberger, K. A Survey and New Measurements of Ice Vapor Pressure at Temperatures between 170 and 250K. *Geophys. Res. Lett.* **1993**, *20* (5), 363−366.
(48) Mauersberger, K. Vapor Pressure above Ice at Temperatures below 170 K. *Geophys. Res. Lett.* **2003**, *30* (3), 1121.
(49) Murphy, D. M.; Koop, T. Review of the Vapour Pressures of Ice and Supercooled Water for Atmospheric Applications. *Q. J. R. Meteorol. Soc.* **2005**, *131* (608), 1539−1565.
(50) Gardner, A. S.; Sharp, M. J. A Review of Snow and Ice Albedo and the Development of a New Physically Based Broadband Albedo Parameterization. *J. Geophys. Res.* **2010**, *115* (F1), F01009.
(51) Pruppacher, H. R.; Klett, J. D. *Microphysics of Clouds and Precipitation;* Reidel: Dordrecht, The Netherlands, 1980. DOI: 10.1007/978-0-306-48100-0
(52) Baker, M. B.; Peter, T. Small-Scale Cloud Processes and Climate. *Nature* **2008**, *451* (7176), 299−300.
(53) Filacchione, G.; De Sanctis, M. C.; Capaccioni, F.; Raponi, A.; Tosi, F.; Ciarniello, M.; Cerroni, P.; Piccioni, G.; Capria, M. T.; Palomba, E.; Bellucci, G.; Erard, S.; Bockelee-Morvan, D.; Leyrat, C.; Arnold, G.; Barucci, M. A.; Fulchignoni, M.; Schmitt, B.; Quirico, E.; Jaumann, R.; Stephan, K.; Longobardo, A.; Mennella, V.; Migliorini, A.; Ammannito, E.; Benkhoff, J.; Bibring, J. P.; Blanco, A.; Blecka, M. I.; Carlson, R.; Carsenty, U.; Colangeli, L.; Combes, M.; Combi, M.; Crovisier, J.; Drossart, P.; Encrenaz, T.; Federico, C.; Fink, U.; Fonti, S.; Ip, W. H.; Irwin, P.; Kuehrt, E.; Langevin, Y.; Magni, G.; McCord, T.; Moroz, L.; Mottola, S.; Orofino, V.; Schade, U.; Taylor, F.; Tiphene, D.; Tozzi, G. P.; Beck, P.; Biver, N.; Bonal, L.; Combe, J.-Ph.; Despan, D.; Flamini, E.; Formisano, M.; Fornasier, S.; Frigeri, A.; Grassi, D.; Gudipati, M. S.; Kappel, D.; Mancarella, F.; Markus, K.; Merlin, F.; Orosei, R.; Rinaldi, G.; Cartacci, M.; Cicchetti, A.; Giuppi, S.; Hello, Y.; Henry, F.; Jacquinod, S.; Reess, J. M.; Noschese, R.; Politi, R.; Peter, G. Exposed Water Ice on the Nucleus of Comet 67P/Churyumov−Gerasimenko. *Nature* **2016**, *529* (7586), 368−372.
(54) del Rosso, L.; Celli, M.; Colognesi, D.; Grazzi, F.; Ulivi, L. Irreversible Structural Changes of Recovered Hydrogen Hydrate Transforming from C_0 Phase to Ice XVII. *Chem. Phys.* **2021**, *544*, 111092.
(55) Bachler, J.; Giebelmann, J.; Amann-Winkel, K.; Loerting, T. Pressure-Annealed High-Density Amorphous Ice Made from Vitrified Water Droplets: A Systematic Calorimetry Study on Water's Second Glass Transition. *J. Chem. Phys.* **2022**, *157* (6), 064502.

https://doi.org/10.1021/acs.jpclett.3c00408
J. Phys. Chem. Lett. 2023, 14, 5055−5060